Electronic Supplementary Material (ESI) for Chemical Science.

Supplementary information for:

Atomic structural changes in the formation of transition metal tungstates: The role of polyoxometalate structures in material crystallization

Susanne Linn Skjærvø, Andy S. Anker, Magnus C. Wied, Emil T. S. Kjær, Mikkel Juelsholt, Troels L. Christiansen, Kirsten M. Ø. Jensen*

*Correspondence to kirsten@chem.ku.dk (KMØJ)

Department of Chemistry and Nano-Science Center, University of Copenhagen, 2100 Copenhagen Ø, Denmark

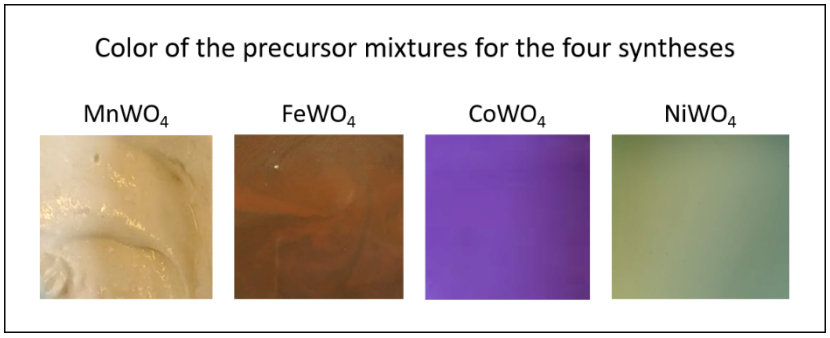

Figure S1: Color of the precursor mixtures, straight after mixing the aqueous solutions of $MCl_2 \cdot xH_2O$ (M = Mn, Fe, Co, Ni) and $Na_2WO_4 \cdot 2H_2O$, prior to heating.

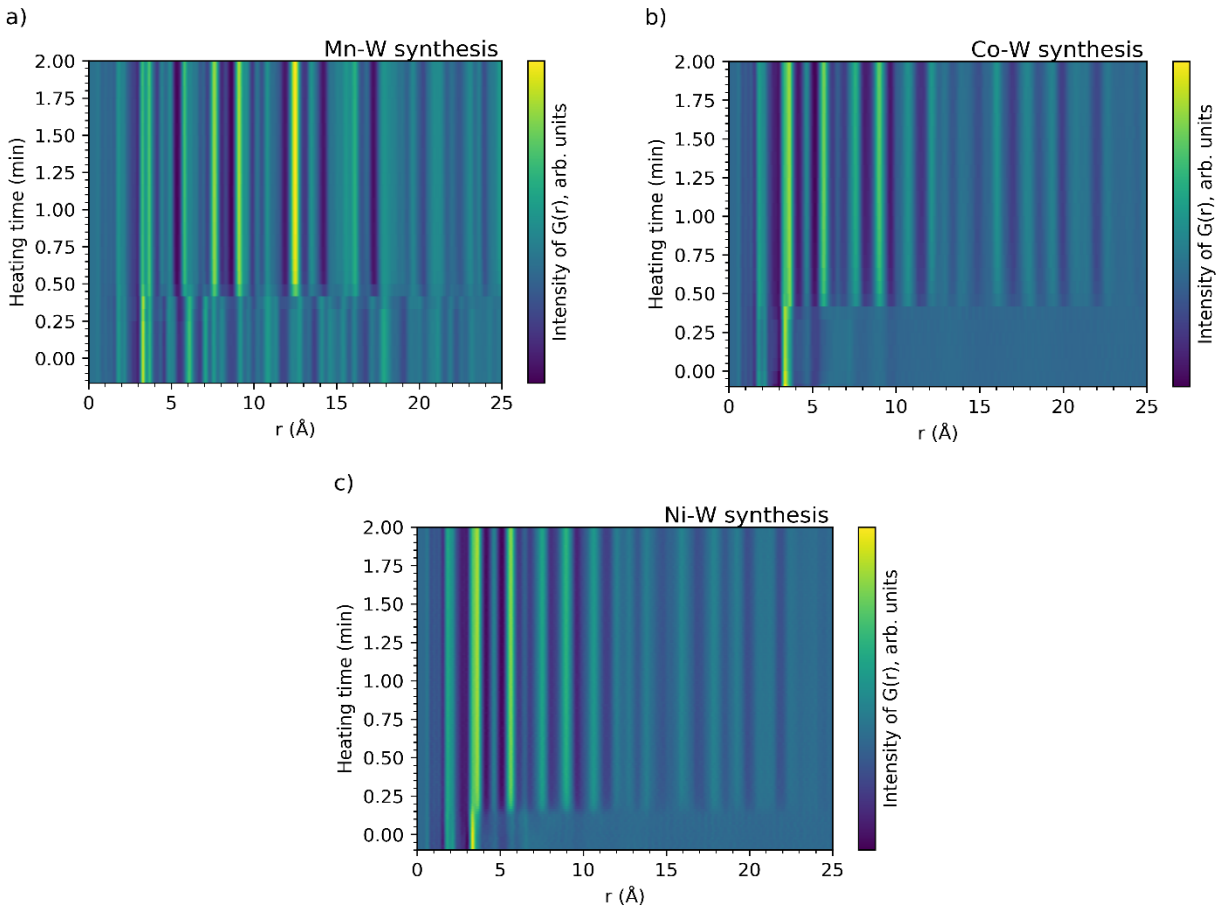

Figure S2: Time-resolved PDFs calculated from *in situ* total scattering data for the a) Mn-W, b) Co-W and c) Ni-W syntheses at 160 °C and 100 bar.

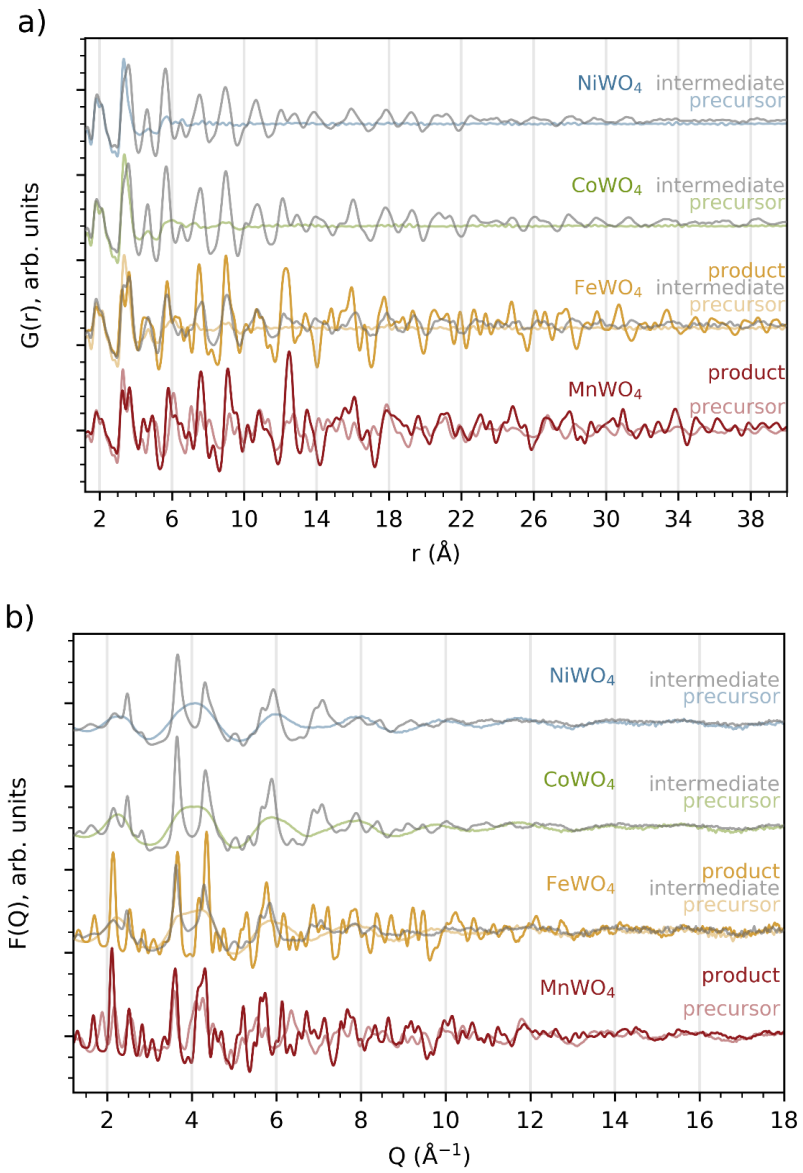

Figure S3: PDFs and b) F(Q) from in situ total scattering data of present phases during the MWO_4 (M = Mn, Fe, Co, Ni) syntheses at 160 °C and 100 bar.

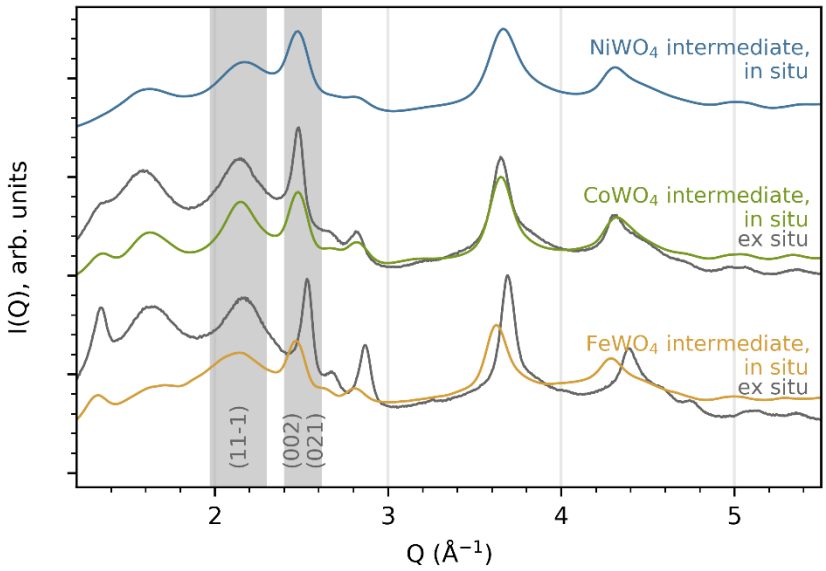

Figure S4: Diffraction pattern of the MWO_4 intermediate phases, obtained both *in situ* and *ex situ*. A selection of diffraction lines from the $FeWO_4$ product phase (ICSD Code 26843[1]) are highlighted in grey areas. Note that the pressure during the *in situ* experiment (100 bar) is higher than for the *ex situ* experiment (1.3 bar).

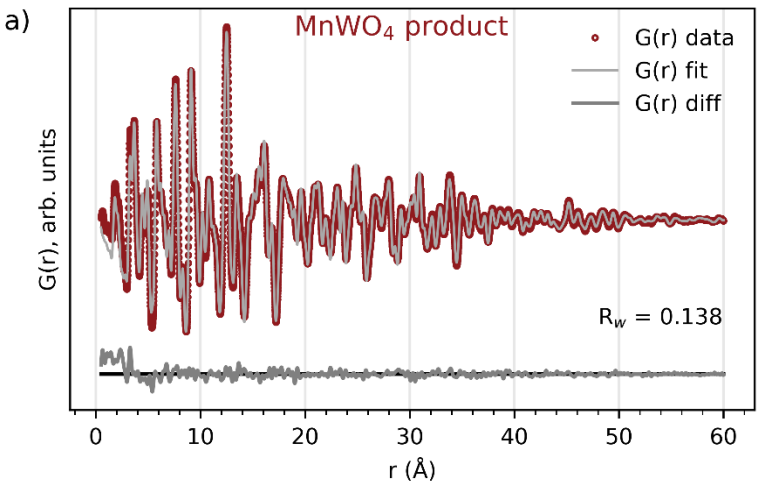

Refined values	
Scale factor	1.10
Unit cell parameters, Å (a, b, c)	4.827, 5.765, 5.001
Anisotropic adp, u_{aniso} (Mn, W, O): u11, u22, u33, u12, u13, u33	0.015, 0.016, 0.015, 0, 0.002, 0 0.007, 0.007, 0.005, 0, 0, 0 0.047, 0.008, 0.064, -0.006, 0.002, 0.004
δ_2	2.11
Crystallite size in Å	1074

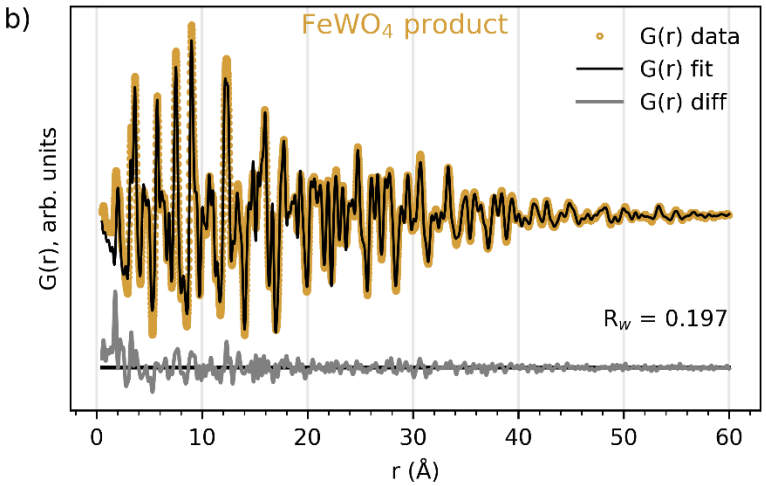

Refined values	
Scale factor	1.00
Unit cell parameters, Å (a, b, c)	4.719, 5.701, 4.973
Anisotropic adp, u_{aniso} (Fe, W, O): u11, u22, u33, u12, u13, u33	0.011, 0.009, 0.010, 0, -0.001, 0 0.008, 0.006, 0.006, 0, -0.001, 0 0.043, 0.022, 0.016, -0.007, -0.007, 0.007
δ_2	3.57
Crystallite size in Å	320

Figure S5: a) Fit of $MnWO_4$ (ICSD Code 67906[2]) and b) $FeWO_4$ (ICSD Code 26843[1]) to PDFs of product from Mn-W and Fe-W syntheses, collected *in situ* after approx. 12 min of heating at 160 °C and 100 bar. Scale factor, unit cell parameters, anisotropic temperature factors, δ_2 and crystallite size were refined, as listed in the tables.

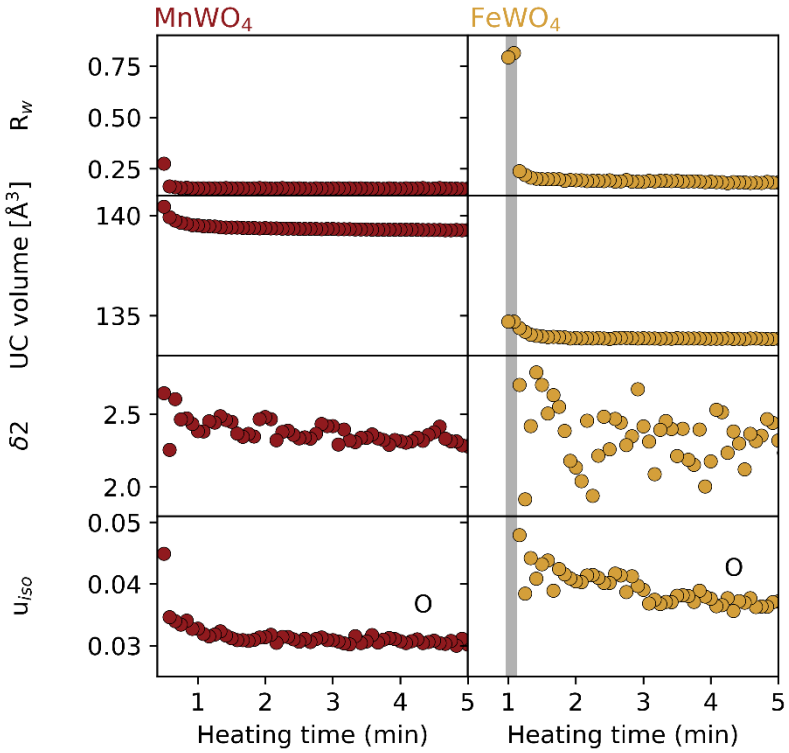

Figure S6: Results from reverse sequential real space Rietveld refinements of $MnWO_4$ (ICSD Code 67906[2]) and $FeWO_4$ (ICSD Code 26843[1]) structures to the PDFs in the range 1.3 – 60 Å, obtained from *in situ* total scattering. The R_w value of the fits, unit cell volume (Å^3), δ2 and isotropic ADPs (u_{iso}) of O is shown. The vertical line in the middle of the plots indicate a changing time-scale. The area where the $FeWO_4$ intermediate phase is present, is highlighted with grey color.

Refined values	
Scale factor	0.814
Unit cell parameters, Å (a, b, c, β)	4.682, 5.625, 5.112, 91.3
ΔCo_y, ΔW_y	0.0462 (fixed), 0.0473 (fixed)
Isotropic ADPs, u_{iso} (Co, W, O)	0.019, 0.012, 0.028
δ_2	2.395

Refined values	
Scale factor	1.002
Unit cell parameters, Å (a, b, c, β)	4.649, 5.630, 5.225, 88.3
ΔCo_y, ΔW_y	0.0184, 0.0309
Isotropic ADPs, u_{iso} (Co, W, O)	0.014, 0.017, 0.039
δ_2	2.626

Table S1: Refined values of the fits of wolframite-$CoWO_4$ [3] to the $CoWO_4$ intermediate phase, a) without and b) with refining the atomic positions of Co and W. The fits are shown in Figure 5 of the main paper.

a)

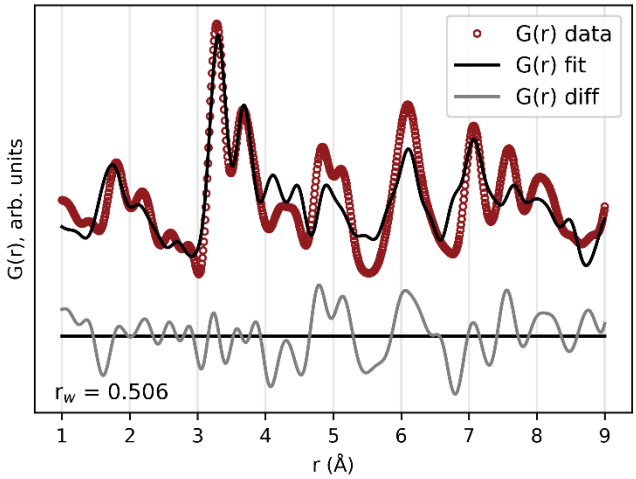

b)

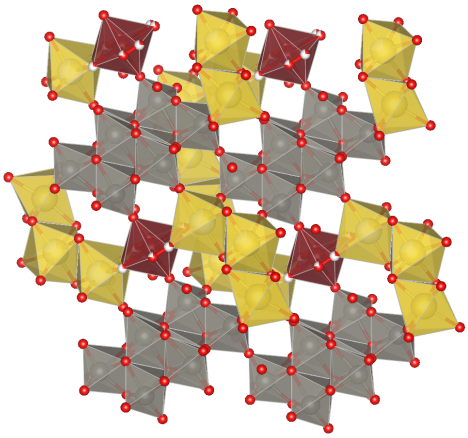

Refined values	
Scale factor	0.789
Unit cell parameters, in Å (a, b, c, α, β, γ)	9.372, 10.162, 10.757, 104.3, 102.0, 99.1
Isotropic adp, B_{iso} (W, Mn, Na, O)	0.194, 0.005, 0.005, 0.185
δ_2	1.22e-04

Figure S7: a) Fit of $Na_4Mn[Mo_8O_{27}]\cdot 20H_2O$ (COD 4031570)[4], to PDF of crystalline Mn-W precursor phase, measured in situ before heating was initiated. Scale factor, unit cell parameters, isotropic temperature factors and δ_2 were refined. b) A representative view of the structure, with Mn, W, Na and O in dark red, grey, yellow and bright red, respectively.

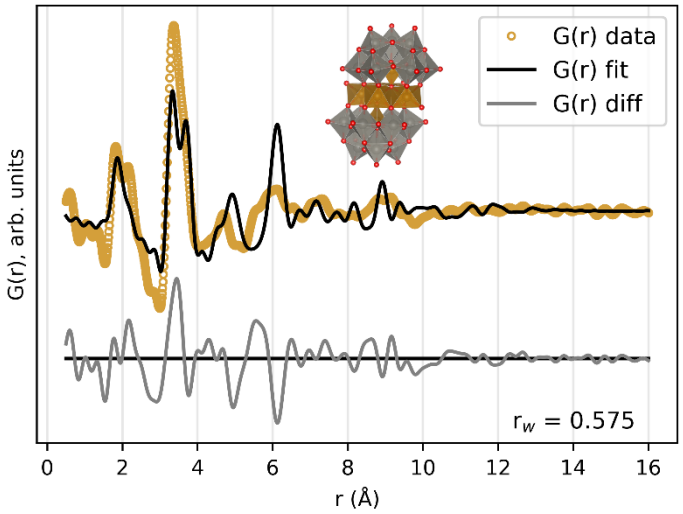

Refined values	
Scale factor	1.13
Zoom for cluster (x, y, z)	97.2 % 99.3 % 103.1 %
Isotropic adp, B_{iso} (W, Fe) (Å^2)	0.3 (upper bound) 0.001 (lower bound)
δ_2 (Å)	0.50 (lower bound)

Figure S8: Fit of extracted sandwich cluster from $Na_{16}(Fe_4(H_2O)_2(FeW_9O_{34})_2)(H_2O)_{46}$ by Barats et al.[5] to the PDF of the mixed $FeWO_4$ precursor paste, obtained from total scattering data measured in situ before heating was initiated. Scale factor, zoom factor for the cluster related to the crystallographic directions of the parent crystal structure, isotropic temperature factors and δ_2 were refined.

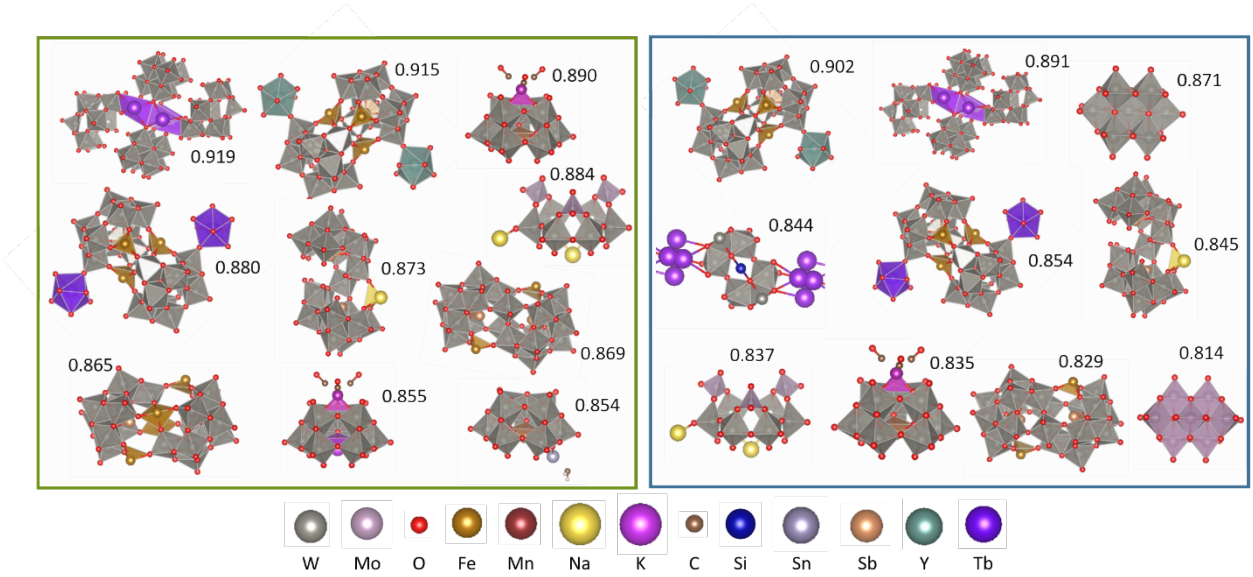

Figure S9: The ten structures giving the highest Pearson correlation with the experimental PDF from $CoWO_4$ (green frame) and $NiWO_4$ (blue frame) precursors. All relevant clusters were extracted from structures in the COD + ICSD databases and compared to the PDF of the $CoWO_4$ and $NiWO_4$ precursor phases in the range 1-5 Å. Correlation coefficients are placed next to each structure. The structure visualizations were done with VESTA.[10]

a)

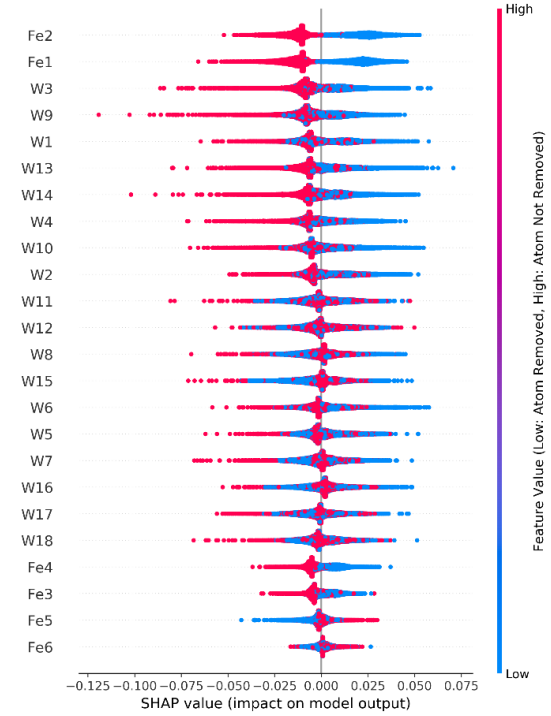

b)

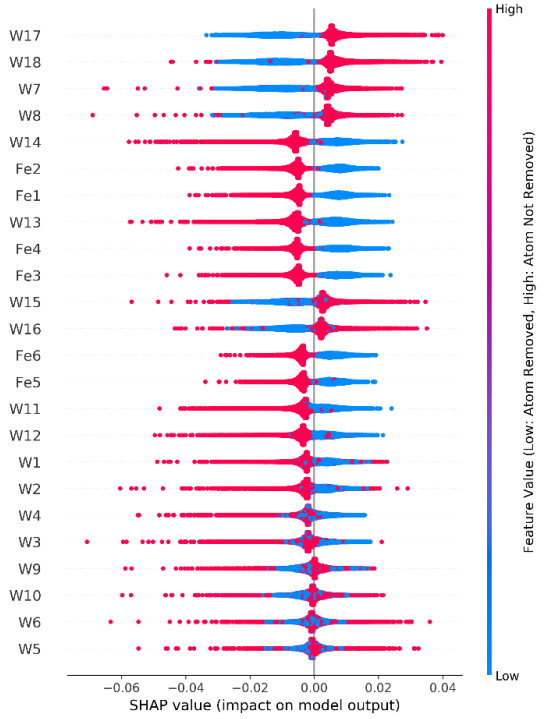

c)

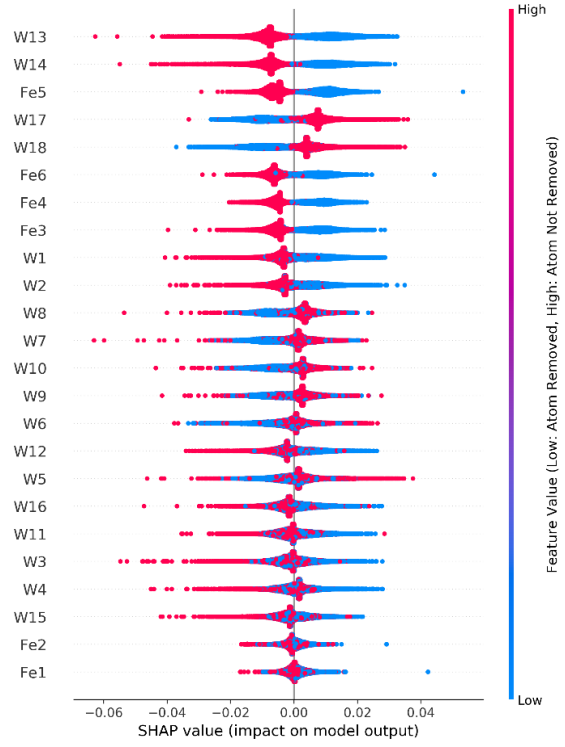

Figure S10: Summary plot of the calculated SHAP values for datasets representing a) precursor before heating, b) intermediate after 1.1 min heating and c) product phase after 1.35 min of heating.

For all the metal atoms, each of the 10000 fits fed to the machine learning algorithm are represented as a data point. If the data point is blue, it means that the respective fit does not contain this atom, and the opposite is true for red data points. Every data point's position along the x-axis in the plot (SHAP value) tells us the effect of this atom's presence (or non-presence) on the R_{wp} value. A large absolute value on the SHAP value means that the metal atom is deemed important by the algorithm, and the sign of the SHAP value tells us whether it has a good (minus) or bad (plus) effect on the R_{wp} value.

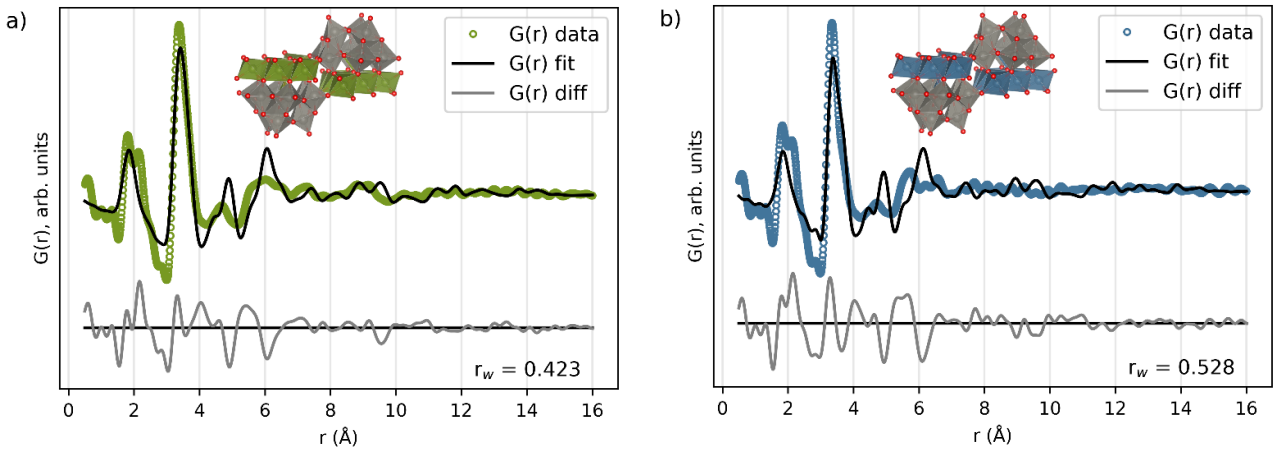

Figure S11: Fits of the skewed cluster $(M_6(MW_9O_{34}))_2$ where M = Co, Ni, stemming from the $(Ni_6(H_2O)_9(OH)_3(HSiW_9O_{34}))_2(H_2O)_{12}$ structure[11] to the $CoWO_4$ and $NiWO_4$ precursor PDFs. Scale factor, zoom factor for the cluster related to the crystallographic directions of the parent crystal structure, isotropic temperature factors and δ_2 were refined.

Detailed description of the Motif Extraction using machine learning

Time-resolved PDF modelling: Automated motif extraction using machine learning

We wanted to investigate if motifs from the typical sandwich cluster in could describe our precursor structure, and how far into the reaction these motifs would persist. We did this using the ML-MoTeX method for analysis of automated PDF modelling.[6] The method is described in detail by Anker et al. The Fe-containing tungstate sandwich cluster described by Barats et al.[5] was chosen as the starting model for our investigations. H_2O and Na^+ were removed from the structure, and only one whole sandwich cluster with the formula $[Fe_4(FeW_9O_{34})_2]^{16-}$ was left, which we used as a discrete model for PDF fitting. Using this starting model, we created a catalogue of fragments by removing metal atoms (and oxygen bonded to them) in a random fashion from the parent cluster. As the chosen parent cluster contains 24 metal atoms, producing and fitting all possible 2^{24} - 1 = 16,777,215 cluster configurations to a PDF would be computationally expensive. However, the machine learning method allows to obtain structural information by creating a fraction of these structures. 10,000 random configurations were thus produced and fitted to the PDFs in the range 1.5 – 6.8 Å. The scale factor, isotropic atomic displacement parameters and a parameter relating to the correlated atomic motion (δ_2)[7] were refined. The structures were also allowed to expand/shrink up to 1 % of their original size. The results of these fits were then used to train a machine learning (ML) algorithm using Gradient Boosting Decision Trees (GBDT).[8] The GBDT method does the regression task of predicting the R_{wp} value of a fit based on the structural input. The effect of each atom in the structure was interpreted using SHAP (SHapley Additive exPlanation) values.[9] The amplitude of the SHAP value quantifies the importance of an atom's presence in the

structure, while the sign of the SHAP value tells whether an atom's presence elevates or decreases the R_{wp} value of the fit. This process was done for the entire $FeWO_4$ in situ series, to see if motifs from the sandwich cluster could describe all the phases present during the reaction. In order to compress the information further and see trends in the in situ series, the mean and standard deviation of each atom's SHAP values were calculated. These values were then plotted as a function of time, revealing which metal atoms are deemed by the algorithm to contribute to the fits in a significant way.

References

1 D. Ülkü, *Z. Kristallogr. - New Cryst. Struct.*, 1967, **124**, 192–219.

2 J. Macavei and H. Schulz, *Z. Kristallogr. - New Cryst. Struct.*, 1993, **207**, 193–208.

3 H. Weitzel, *Zeitschrift für Krist. - Cryst. Mater.*, 1976, **144**, 238–258.

4 S. J. Angus-Dunne, J. A. Irwin, R. C. Burns, G. A. Lawrance and D. C. Craig, *J. Chem. Soc., Dalton Trans.*, 1993, **1993**, 2717–2726.

5 D. Barats, G. Leitus, R. Popovitz-Biro, L. J. W. Shimon and R. Neumann, *Angew. Chem., Int. Ed.*, 2008, **47**, 9908–9912.

6 T. Lindahl Christiansen, E. T. S. Kjær, A. Kovyakh, M. L. Röderen, M. Høj, T. Vosch and K. M. Ø. Jensen, *J. Appl. Crystallogr.*, 2020, **53**, 148–158.

7 I.-K. Jeong, T. Proffen, F. Mohiuddin-Jacobs and S. J. L. Billinge, *J. Phys. Chem. A*, 1999, **103**, 921–924.

8 T. Chen and C. Guestrin, in *Proceedings of the 22nd ACM SIGKDD International Conference on Knowledge Discovery and Data Mining*, 2016, pp. 785–794.

9 S. Lundberg and S.-I. Lee, *ArXiv*.

10 K. Momma and F. Izumi, *J. Appl. Cryst.*, 2011, **44**, 1272–1276.

11 X.-M. Luo, L. Chen, Y.-Y. Dong, J. Li, C.-H. Cui, J.-P. Cao and Y. Xu, *Dalt. Trans.*, 2018, **47**, 9504–9511.